Rock Engineering and Rock Mechanics: Structures in and on Rock Masses – Alejano, Perucho, Olalla & Jiménez (Eds)

Mining induced static stress transfer and its relation to a high-precision located $M_w = 1.9$ seismic event in a South African gold mine

M. Ziegler
Helmholtz Centre Potsdam, GFZ German Research Centre for Geosciences, Potsdam, Germany; University of Potsdam, Potsdam, Germany

K. Reiter & O. Heidbach
Helmholtz Centre Potsdam, GFZ German Research Centre for Geosciences, Potsdam, Germany

A. Zang
Helmholtz Centre, GFZ German Research Centre for Geosciences, Potsdam, Germany; University of Potsdam, Potsdam, Germany

G. Kwiatek
Helmholtz Centre, GFZ German Research Centre for Geosciences, Potsdam, Germany

T. Dahm & G. Dresen
Helmholtz Centre, GFZ German Research Centre for Geosciences, Potsdam, Germany
University of Potsdam, Potsdam, Germany

G. Hofmann
Anglogold Ashanti, South Africa

ABSTRACT: On 27 December 2007 a M_w 1.9 seismic event occurred in the Mponeng gold mine, South Africa. The seismic event's hypocentre, as well as the fore- and aftershocks were located with the JAGUARS acoustic emission array, placed at mining level 116. Thus, hypocentre depth (3509 m) and focal mechanism are very well constrained. Since no mining activity took place more than two days before the event, dynamic triggering due to blasting is ruled out. We investigate the hypothesis that static stress transfer due to excavation of the gold reef induced the event. To estimate these mining-induced stress changes, we set up a small scale ($450 \times 300 \times 310\,m^3$) high resolution 3D geomechanical-numerical model, containing most of the seismic events detected. The model is made of the four different rock units present in the mine: quartzite (footwall), hard lava (hanging wall), conglomerate (gold reef), and diorite (dykes). The virgin in-situ stress, determined in nearby TauTona mine, is used to implement initial conditions. Elastic rock properties are taken from laboratory measurements. For the numerical solution, we are using the finite element method, with a discretised mesh of ~1 million elements. From the computed 3D stress tensor we estimate the Coulomb failure stress change (ΔCFS) on the fault plane of the event in two ways: The first with shear stresses resolved in rake direction (ΔCFS_{slip}) and the second using the maximum shear stress (ΔCFS_{max}) on the plane. The ΔCFS_{slip} values are negative, indicating that, according to the model, mining activity brought slip in the resolved direction on the resolved fault plane further away from failure. Considering model uncertainties with respect to fault plane geometry, rake vector, and elastic parameters, this result remains stable. In contrary, the ΔCFS_{max} value is positive, indicating that, given the modelled stress is correct, a high potential for triggering a rupture is available.

1 INTRODUCTION

On 27 December 2007, a $M_w = 1.9$ seismic event occurred in the ultra-deep levels of Mponeng gold mine, Carletonville, South Africa. The hypocentre and its aftershocks were located in a depth of 3,509 m, in direct proximity (<100 m) to recently mined out areas, access tunnels and a dyke (Fig. 1) (Kwiatek et al. 2010; Kwiatek & Ben-Zion 2013).

The Mponeng gold mine represents a typical ultra-deep tabular mining environment. The mine is located in Witwatersrand Basin, one of the world's largest gold mining areas. Mponeng mine exploits c. 1 m high, c. 22° dipping Ventersdorp Contact Reef (VCR) to a depth of currently down to c. 3,900 m (AngloGold Ashanti Limited, 2013; Plenkers, 2010; Roberts & Schweitzer, 1999). The hanging wall is composed of hard lava, while the footwall consists of quartzite

(Malan, 1999). About 5–10 % of Witwatersrand Basin are made of various dykes and sills (Pretorius, 1976). Two almost vertically dipping diorite-gabbro dykes are in close proximity to the seismic event's hypocentre (Kwiatek et al., 2010). From Figure 1 it is evident that the hypocentre of the $M_w = 1.9$ seismic event was located within one of the two dykes, the Pink-Green dyke (Yabe et al., 2009).

Such induced seismicity is a known phenomenon in mines, especially in deep level mines. This is due to high overburden stresses and the presence of dykes promoting rock failure (Gay, 1979; Pretorius, 1976). In most cases the rock is not critically stressed before the mining. Hence, failure is primaryly a result of the removal of material from the mine, which induces static stress changes. As soon as the stresses reach the strength of the rock, failure occurs.

Here we investigate the hypothesis whether the static stress transfer due to mass removal induced the M_w=1.9 seismic event in the Mponeng gold mine. In particular we estimate the stress changes at the hypocentre using the Coulomb failure criterion. The calculation of the stress changes is accomplished by means of a 3D geomechanical-numerical model that represents the main geometrical and structural features of the gold mine at that particular depth.

Data on the progress of mining is available from the gold mine company Anglogold Ashanti and from the JAGUARS-group (Japanese-German Underground Acoustic Research in South Africa). The data shows a consecutive removal of material from the gold reef in monthly steps for 2007 and 2008. This mining progress of the gold reef is included in the geometry of Mponeng mine.

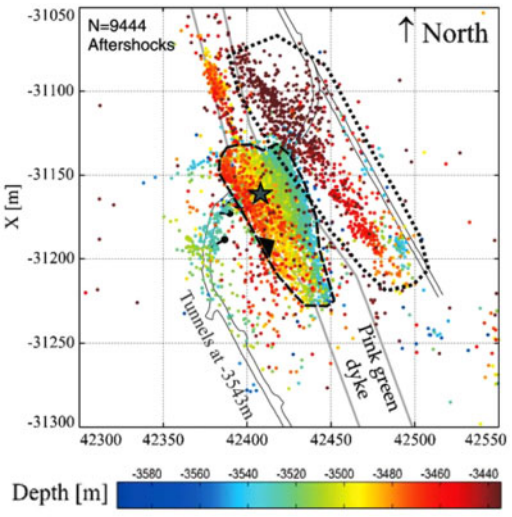

Figure 1. Distribution of aftershocks of the $M_w = 1.9$ seismic event, colour-coded according to their depths. The aftershocks on the fault plane are within the dashed black linlocation of the hypocentre is shown by the black star (Kwiatek et al., 2010).

2 GEOMECHANICAL-NUMERICAL MODEL

In the course of the model set up we made the following simplifying assumptions:

1. *Elasticity*. We assume that the rock material behaves linear and that the elastic properties are isotropic and homogeneous in each material block (gold reef, dyke, and host rock). Thus, the elastic response can be described with the Young's Modulus E and the Poisson ratio ν (Table 1).
2. *Plasticity*. The roof of the mined out area is subject to plastic deformations (Malan, 1999). However, these deformations and the resulting stress changes have a small impact compared to the induced changes of the elastic response, and hence are disregarded. In this sense the fully elastic response in the far-field is an overestimation of the static stress changes as the energy that is dissipated in the near-field due to plastic deformation is neglected
3. *Backfill*. A slurry of waste material is pumped into the mined out areas (Lucier et al., 2009). However, the rigidity of the backfill is negligibly small compared to that of the mined out rock. Hence, backfill is not regarded.
4. *Support pillars/Props*. They are of steel or wood and support the roof of the mined out areas. However, only very local effects on the stress field can be expected and thus we do not model these pillars.
5. *Thermal stresses*. According to Jones (1988) the temperature in focal depth is about 60°C. The air temperature in the mine is cooled down to about 35°–40°C. The stresses induced by the mentioned temperature change are at least one order of magnitude smaller than stress changes by mass removal. Hence they are not regarded.
6. *Dynamic triggering*. During the Christmas holidays, no blasting was performed at the time and the days before the $M_w = 19$ event. Thus, dynamic triggering can be ruled out.
7. *Gravity acceleration*. We assume gravitational body forces of 9.79 m/s^2 for the model volume.
8. *Secondary processes* We do not implement any secondary processes such as subcritical fracture growth at the tip of the mining front. This is a potential major source of systematic uncertainty of the model.

With these assumptions we have to solve the partial differential equation of the equilibrium of forces with linear-elastic rheology. Due to the complexity of the 3D geometry and the inhomogeneous distribution of material properties, we use the Finite Element Method (FEM) to solve the problem numerically at discrete points. The FEM with its unstructured mesh allows the discretisation of a volume with a high resolution in the area of interest and a coarse mesh further away. Furthermore, the FEM is capable to resemble the irregular shapes of the tunnel system, dykes and the thin gold reef.

Table 1. Elastic material properties an density applied in the model (Gay, 1979; Gercek, 2007; Malan, 1999; MatWeb LLC, 2013).

Lithology	Young's modulus [GPa]	Poisson ratio	Density [kg/m^3]
Hanging Wall	88	0.26	2,902
Footwall	79	0.13	2,710
Dykes	110	0.25	2,900
Gold reef	69	0.20	2,600

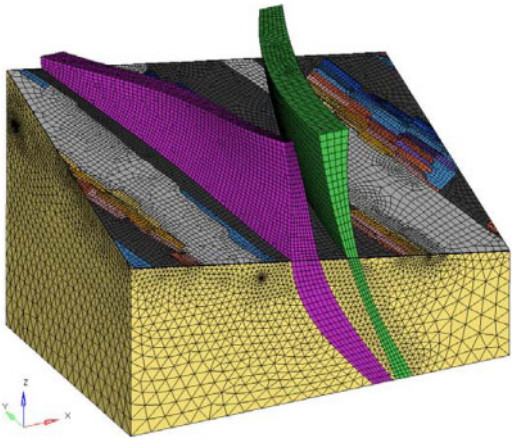

Figure 2. The discretised geometry of the gold mine. The gold reef is color-coded according to the progress of the mining. The hanging wall is omitted here to facilitate viewing. Y-axis points to the north. The mesh contains approximately one million hexahedron and tetrahedron elements.

The model volume of $450 \times 300 \times 310\,\mathrm{m}^3$ is only a small part of the mine that is located around the hypocentre of the $M_w = 1.9$ seismic event. To ensure that the final discretisation of the volume is sufficiently fine and to avoid any substantial numerical errors, we performed a series of 2D resolution test models (not shown in this paper). The resulting 3D mesh is presented in Figure 2 and 3. The kinematic boundary conditions of the models are determined in a way that they represent the overburden and that the resulting stress field matches the in-situ stress data from the neighbouring gold mine TauTona; data are presented by Lucier et al. (2009). However, for our calculation of the stress changes only, this calibration is actually not of great importance as the initial stress field of the model is eliminated during the calculation of ΔCFS (see Section 3). Only for a more advanced study (plasticity, secondary processes) the initial stress field calibration is of great importance, but this is not the focus of this paper.

In the 3D geomechanical-numerical model, the mined out areas are removed in consecutive monthly steps. The instant elastic response and the resulting 3D stress tensor are computed at every integration point

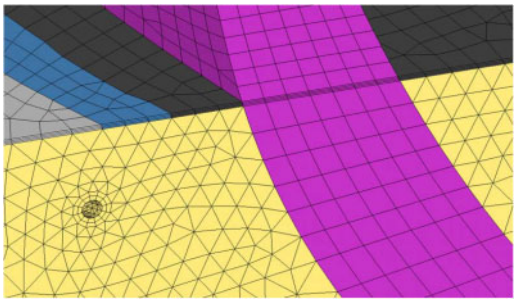

Figure 3. Close-up of the discretised geometry. The Pink-Green dyke, the thin layered gold reef and the finer discretisation around a mining tunnel are visible.

within the model for each step of mass removal. In the following analysis, scalar values are derived from the stress tensor with its six independent components.

3 MODEL RESULTS

To analyse the resulting stress changes we use the Coulomb criterion to derive scalar values. According to Jaeger and Cook (1971) and King et al. (1994), Coulomb failure stress (CFS) quantifies the stress change with respect to an arbitrarily oriented plane, e.g. the rupture plane of an earthquake. Expressed in a formula this is:

$$CFS = \tau - (\mu \sigma_n + C_0) \tag{1}$$

where τ is the shear stress, μ the friction coefficient, σ_n the normal stress and C_0 the cohesion. CFS is always computed for a given plane and we use here the rupture plane of the $M_w = 1.9$ event with 348|56 (strike|dip) (Kwiatek & Ben-Zion 2013). The changes in CFS (ΔCFS) show whether a fault is brought closer to, or further away from failure. ΔCFS is calculated by the subtraction of CFS (Step1) of the unmined stress state of the model, from CFS (StepX) for the elastic response of the model at a certain time step. Two different approaches are chosen to calculate ΔCFS from the same resulting stress tensors.

In the first approach, CFS is computed, using the shear stress resolved in the direction of the slip of the seismic event (CFS_{slip}). According to Kwiatek & Ben-Zion (2013) the slip is −59°. The second approach uses the maximum shear stress on the plane (CFS_{max}).

ΔCFS_{slip} in the area around the hypocentre of the seismic event is negative (Fig. 4). That means the area is brought away from failure, compared to an unmined stress state. Hence, according to ΔCFS_{slip}, the model does not explain the occurrence of the $M_w = 1.9$ seismic event.

On the other hand, ΔCFS_{max} in the area around the hypocentre is positive (Fig. 5). That means the area is closer to failure than in an unmined stress state. Hence, using this approach to analyse the model explains the occurrence of the seismic event.

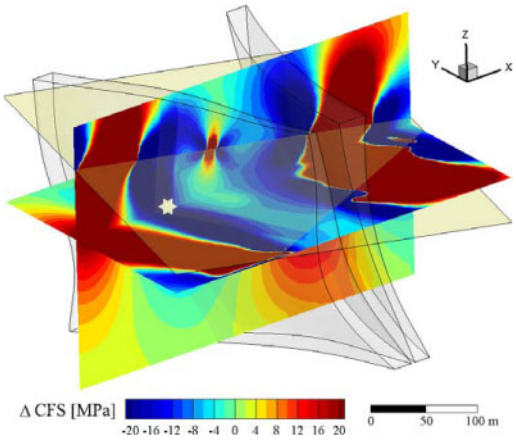

Figure 4. ΔCFS in slip direction (ΔCFS_{slip}) at the time of the $M_w = 1.9$ seismic event. Displayed are two planes that intersect at the hypocentre of the seismic event. Event location is given by the white star. Dykes are the grey compounds and the gold reef is indicated by the yellow dipping plane. Y-axis points to the north. A detailed map view of this result is given in the supplementary figure S1.

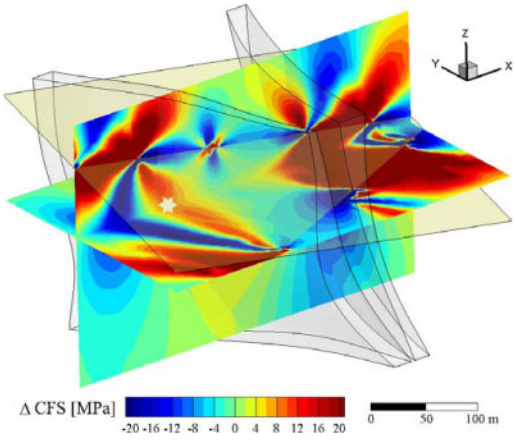

Figure 5. ΔCFS calculated with the maximum shear stress on the rupture plane (ΔCFS_{max}) at the time of the $M_w = 1.9$ seismic event. Displayed are two planes that intersect at the hypocentre of the seismic event. Event location is given by the white star. Dykes are the grey compounds and the gold reef is indicated by the yellow dipping plane. Y-axis points to the north. A detailed map view of this result is given in the supplementary figure S2.

These results suggest a large difference in slip direction of the $M_w = 1.9$ seismic event and the maximum shear stress on the rupture plane at the hypocentre. Indeed, the direction of the latter is derived from the model to be c. 110°. This is in strong contrast to the resolved slip in the direction of −59° on the plane, as displayed in Fig. 6.

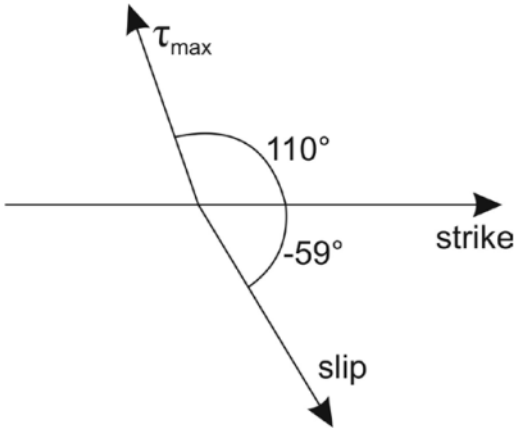

Figure 6. Comparison of the direction of slip on the assumed rupture plane to the maximum shear stress τ_{max} on that fault.

4 DISCUSSION

Based on the analysis of the classical approach amongst seismologist using the ΔCFS_{slip} (Harris et al., 1998; Stein et al., 1999; Heidbach and Ben-Avraham, 2007, Nalbant et al., 1998; Lorenzo-Martin et al., 2007) we have to reject the hypothesis that the stress changes due to the mass removal during mining induced the event. However, at the same time the model clearly shows that the stress changes are significant and reach values of >10 MPa. Possible causes for the failure of the model are the model uncertainties. These are listed in the following, according to their impact on the ΔCFS calculations (the uncertainties have the same impact regardless whether ΔCFS_{max} or ΔCFS_{slip} is used):

- Missing or erroneous extent of mining compartments in the vicinity of the hypocentre.
- Geometry of the gold reef and its rolling behaviour is not included in the model.
- Geometry of the dykes is constructed from a limited number of data points. Only an approach to the actual geometry is realised, but the impact on the stress field is small.
- Assumed rupture plane orientation; ΔCFS is quite sensitive to changes in orientation. Changes can account for several MPa. However, the uncertainty is small given the high precision of the installed seismological network.
- Material properties are gathered from various sources. It is not clear whether all of the applied parameters are elastic. However, testing showed that a large effect of the material properties on the results can be ruled out.
- Some tunnels, box holes and other small features where omitted. However, the impact on the far field stress field is small.
- Large differences in size of adjacent elements exist. However, our test models showed that this influence on the results is minor.

From this list only the first uncertainty is capable to produce a substantial change in the ΔCFS calculation that would be sufficient to change the interpretation. However, as these data are confirmed and double checked by the gold mine company this seems to be very unlikely, too.

Considering the alternative way for the ΔCFS calculation, i.e. using the ΔCFS_{max}, the value is positive in the proximity of the hypocentre. Thus the event could have been induced by stress changes due to mining activity when maximum shear stress on the rupture plane is used. However, the large contrast in the direction of maximum shear stress and slip direction is peculiar. Following the assumption that co-seismic slip should occur in the direction of maximum shear stress, our modelled maximum shear stress on the rupture plane should be at least in the overall direction of the anticipated slip direction. This is not the case in our study (Fig. 6).

Hence, the question arises, whether the computation of ΔCFS, by applying the shear stress in slip direction, is applicable for a mining environment in the first place. Therefore the possibility of the occurrence of additional processes, induced by stress changes, has to be considered. This opens the wide field of fracture mechanics, researching alternative processes which allow inducing a seismic event with a slip in a different direction than the maximum shear stress on the plane. One of those processes is Ortlepp shear. In principle the model is capable to be extended in that way as the incorporated FEM software package Abaqus v6.11 has a wide range of plastic rheologies implemented (Abaqus, 2011). However, to simulate the fracture propagation the computing would increase from one hour to several days taking into account that adaptive meshing to trace the rupture propagation needs to be considered.

5 CONCLUSION

In order to investigate the hypothesis, that the $M_w = 1.9$ seismic event on 27 December 2007 in the deep level Mponeng gold mine near Carletonville, South Africa, was induced by mining activity, a small scale (c. 0.05 km^3) three dimensional geomechanical-numerical model of the gold mine was built, solved and analysed.

The change of Coulomb failure stress at the hypocentre of the seismic event is negative (c. −18 MPa), when the shear stress is resolved strictly in rake direction. However, the change of Coulomb failure stress is positive (c. 9 MPa), when resolved in direction of maximum shear stress. The rake direction is −59°, while the direction of maximum shear stress is 110°, and therefore almost opposed to the rake direction. The first approach to compute the Coulomb failure stress is believed to be correct. Hence, the primary result is that according to the model, the seismic event on 27 December 2007 was not induced by mining activity. The uncertainties in the order of approximately ±1 MPa do not change this result. Further investigations are necessary, to confirm the applicability and the described approach to the computation of the CFS analysis in mining environments.

It is obvious that the $M_w = 1.9$ seismic event was induced by stress changes due to mining activity. There are two possibilities, explaining the failure of the model to show this: The derived focal mechanism could be wrong, but this is highly unlikely, given the quality of the network. The seismic event could have been induced by additional processes, induced by stress changes due to the mining excavations, e.g. Ortlepp shear, which are not included in the model.

ACKNOWLEDGEMENT

The authors would like to thank AngloGold Ashanti for the permission to work and publish the data of Mponeng gold mine, and the JAGUARS group for the provision of the data.

REFERENCES

Abaqus (2011), Abaqus Analysis User's Manual, Version 6.11, *Dassault Systémes Simulia Corp*., Providence, RI, USA.

AngloGold Ashanti Limited. (2013). *Mineral resource and ore reserve report 2012* (p. 177). Newtown, South Africa: Available from: www.aga-reports.com. Retrieved from www.aga-reports.com

Gay, N. C. (1979). The state of stress in a large dyke on ERPM, Boksburg, South Africa. *International Journal of Rock Mechanics and Mining Sciences & Geomechanics*, 16, 179–185. Retrieved from http://www. sciencedirect.com/science/article/pii/0148906279904832

Gercek, H. (2007). Poisson's ratio values for rocks. *International Journal of Rock Mechanics and Mining Sciences & Geomechanics*, 44(1), 1–13. doi:10.1016/j.ijrmms.2006.04.011

Jaeger, J. C., & Cook, N. G. W. (1971). *Fundamentals of Rock Mechanics* (1st ed., p. 515). London: Chapman and Hall Ltd.

Jones, M. Q. W. (1988). Heat flow in the Witwatersrand Basin and environs and its significance for the South African Shield Geotherm and lithosphere thickness. *Journal of Geophysical Research*, 93(B4), 3243–3260. doi:10.1029/JB093iB04p03243

Harris, R. A. (1998), Introduction to special section: Stress triggers, stress shadows, and implications for seismic hazard, *J. Geophys. Res.*, 103, 24347–24358.

Heidbach, O., and Z. Ben-Avraham (2007), Stress evolution and seismic hazard of the Dead Sea fault system, *Earth Planet. Sci. Lett.*, 257, 299–312.

King, G. C. P., Stein, R. S., & Lin, J. (1994). Static stress changes and the triggering of earthquakes. *Bulletin of the Seismological Society of America*, 84(3), 935–953. Retrieved from http://bssa.geoscienceworld.org/content/84/3/935.short

Kwiatek, G., & Ben-Zion, Y. (2013). Assessment of P and S wave energy radiated from very small shear-tensile seismic events in a deep South African mine. *Journal of Geophysical Research: Solid Earth*, 118(7), 3630–3641. doi:10.1002/jgrb.50274

Kwiatek, G., Plenkers, K., Nakatani, M., Yabe, Y., & Dresen, G. (2010). Frequency-Magnitude Characteristics Down to Magnitude −4.4 for Induced Seismicity Recorded

at Mponeng Gold Mine, South Africa. *Bulletin of the Seismological Society of America*, 100(3), 1165–1173. doi:10.1785/0120090277

Lorenzo-Martin, F., F. Roth, and R. Wang (2006), Elastic and inelastic triggering of earthquakes in the North Anatolian Fault zone, *Tectonophysics* (424), 271–289.

Lucier, A. M., Zoback, M. D., Heesakkers, V., Reches, Z., & Murphy, S. K. (2009). Constraining the far-field in situ stress state near a deep South African gold mine. *International Journal of Rock Mechanics and Mining Sciences*, 46(3), 555–567. doi:10.1016/j.ijrmms.2008.09.005

Malan, D. F. (1999). Time-dependent Behaviour of Deep Level Tabular Excavations in Hard Rock. *Rock Mechanics and Rock Engineering*, 32(2), 123–155. doi:10.1007/s006030050028

MatWeb LLC. (2013). MatWeb – Material property data. Retrieved April 10, 2013, from http://www.matweb.com

Nalbant, S. S., A. Hubert, and G. C. P. King (1998), Stress coupling between earthquakes in northwest Turkey and the north Aegean Sea, *J. Geophys. Res.*, 103, 24469–24486.

Plenkers, K., Kwiatek, G., Nakatani, M., & Dresen, G. (2010). Observation of Seismic Events with Frequencies f > 25 kHz at Mponeng Deep Gold Mine, South Africa. *Seismological Research Letters*, 81(3), 467–479. doi:10.1785/gssrl.81.3.467

Pretorius, D. A. (1976). The nature of Witwatersrand gold-uranium deposits. In K. H. Wolf (Ed.), *Handbook of stratabound and stratiform ore deposits – Au, U, Fe, Mn, Hg, Sb, W and P deposits – Volume 7* (p. 656). Amsterdam Oxford New York: Elsevier Scientific Publishing Company.

Roberts, M. K., & Schweitzer, J. K. (1999). Geotechnical areas associated with the Ventersdorp Contact Reef, Witwatersrand Basin, South Africa. *The Journal of the South African Institute of Mining and Metallurgy*, (June 1999), 157–166.

Stein, R. S. (1999), The role of stress transfer in earthquake occurrence, *Nature*, 402, 605–609.

Yabe, Y., Philipp, J., Nakatani, M., Morema, G., Naoi, M., & Kawakata, H. (2009). Observation of numerous aftershocks of an Mw 1.9 earthquake with an AE network installed in a deep gold mine in South Africa. *Earth Planets Space*, 61(10), 49–52.

6 SUPPLEMENTARY MATERIAL

The following two figures show the ΔCFS results for the rupture plane orientation as presented in Figures. Fig. 4 and 5 in map view cutting through the hypocentre of the $M_w = 1.9$ event.

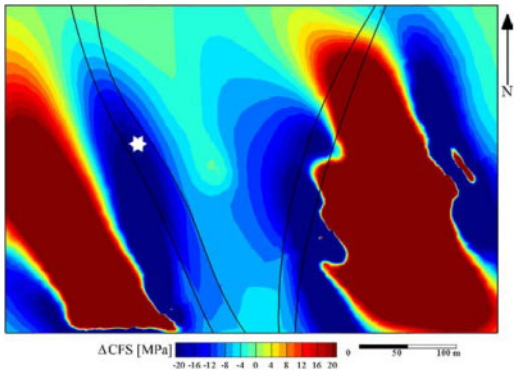

Figure S1. Map view of ΔCFS in slip direction (ΔCFS_{slip}) at the depth of the hypocentre at the time of the $M_w = 1.9$ seismic event. Event location is given by the white star; dykes are the grey lines.

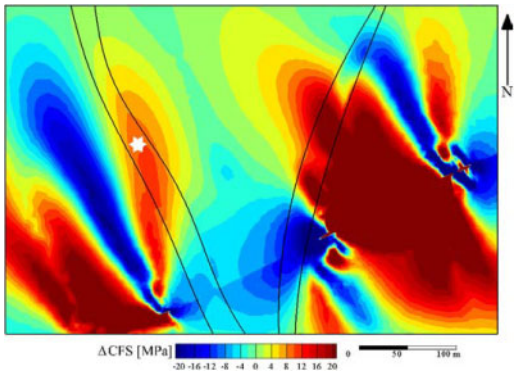

Figure S2. Map view of ΔCFS in direction of maximum shear stress (ΔCFS_{max}) at depth of the hypocentre at the time of the $M_w = 1.9$ seismic event. Event location is given by the white star; dykes are the grey lines.